Power-law Scaling of Turbulence Cospectra for the Stably Stratified Atmospheric Boundary Layer

Yu Cheng • Qi Li • Andrey Grachev • Stefania Argentini • Harindra J.S. Fernando • Pierre Gentine

Received: DD Month YEAR/ Accepted: DD Month YEAR

Abstract Surface turbulent fluxes provide a key boundary condition for the prediction of weather, hydrology, and atmospheric carbon dioxide. The turbulence cospectrum is assumed to typically follow a $-7/3$ power-law scaling, which is used for the high-frequency spectral correction of eddy-covariance data. The derivation of this scaling is mostly grounded on dimensional analysis. The dimensional analysis or cospectral budget analyses, however, can lead to alternative cospectral scaling. Here we examine the shape of turbulence cospectra at high Reynolds number and high wavenumbers based on extensive field measurements of wind velocity and temperature in various stably stratified atmospheric conditions. We show that the cospectral scaling deviates from the $-7/3$ scaling at high wavenumbers in the inertial subrange of the stable atmospheric boundary layer, and appears to follow a -2 power-law scaling. We suggest that -2 power-law

Yu Cheng • Pierre Gentine
Department of Earth and Environmental Engineering, Columbia University, NY, 10027, USA.
E-mail: yc2965@columbia.edu

Qi Li
Department of Civil and Environmental Engineering, Cornell University, NY, 14853, USA.

Andrey Grachev
NOAA Earth System Research Laboratory / Cooperative Institute for Research in Environmental Sciences, University of Colorado, 325 Broadway, R/PSD3, Boulder, CO 80305-3337, USA

Stefania Argentini
Institute of Atmospheric Sciences and Climate, CNR, Rome, Italy.

Harindra J.S. Fernando
Department of Civil and Environmental Engineering and Earth Sciences, University of Notre Dame, IN, 46556, USA.

scaling is a better alternative for cospectral corrections for eddy-covariance measurements of the stable boundary layer.

Keywords Eddy covariance • Stable boundary layer • Surface fluxes • Turbulence cospectra

1 Introduction

Turbulence cospectra of surface fluxes are typically assumed to follow a $-7/3$ power-law scaling in the isotropic inertial subrange (Kolmogorov 1941) according to derivations based on dimensional analysis (Lumley 1964; Lumley 1967). The $-7/3$ power-law scaling has been validated with laboratory experiments (Saddoughi and Veeravalli 1994) and field measurements in the atmospheric boundary layer (e.g., the Kansas experiment) (Kaimal et al. 1972; Wyngaard and Coté 1972). The exact shape of the cospectra is important for field observations as well as theoretical modeling. Indeed, in eddy-covariance (EC) measurements of turbulent fluxes in the atmospheric surface layer (ASL), an assumed cospectral shape is used for the spectral correction of momentum, heat, water vapour and CO_2 fluxes (Moore 1986; Leuning and Moncrieff 1990; Horst 1997; Moncrieff et al. 1997; Aubinet et al. 1999; Massman 2000). Recently, Mamadou et al. (2016) showed that the calculated long-term CO_2 fluxes from EC observation are particularly sensitive to the assumed cospectral shape, and a change of the assumed cospectral correction scaling can even reverse a net terrestrial carbon sink into a source.

Monin and Yaglom (1975) pointed out that Lumley's derivation of the $-7/3$ power-law scaling (Lumley 1964; Lumley 1967) was not sufficiently rigorous and accurate as it relied on the rough approximation (Kovasznay 1948) that the spectral energy transfer rate is only related to the turbulent energy spectrum and wavenumber. In recent years, other slopes of the turbulence cospectra have been reported. In a wind tunnel experiment, an asymptotic -2 power-law scaling was observed for the heat-flux cospectrum (Mydlarski and Warhaft 1998) in stably stratified turbulence at $R_\lambda = 582$, where R_λ is the Taylor-microscale-based Reynolds number. Mydlarski (2003) also found a -2 power-law scaling for heat flux by analyzing both the cospectrum and the heat flux structure function at $R_\lambda = 407$ when a temperature gradient was imposed in the transverse direction, although the study suggested that the slope might increase toward $-7/3$ as Reynolds number increases. Sakai et al. (2008) showed a -2 power-law for radial velocity-concentration cospectrum in a turbulent jet at $R_\lambda = 263$. These observations are still at lower Reynolds numbers than turbulence in the ABL where R_λ typically exceeds 1000 (Table 1) and therefore this raises the question of the exact cospectral shape in the stably stratified atmospheric boundary layer.

Among numerical studies, O'Gorman and Pullin (2005) found a power-law scaling close to -2 in the velocity-scalar cospectrum in a direct numerical simulation (DNS) of homogeneous and isotropic velocity field with a mean scalar gradient at $R_\lambda = 265$. Watanabe and Gotoh (2007) observed a -2 power-law scaling regime to the right side of the $-7/3$ power-law scaling regime in the cospectrum of scalar flux with a high-resolution DNS of isotropic turbulence at $R_\lambda = 585$. In fact, figure 2 in their paper clearly shows that the -2 power-law scaling has a larger plateau compared to the $-7/3$ power-law scaling in the compensated cospectra. Bos et al. (2004) also found a clear -2 power-law scaling in velocity-scalar cospectrum in large eddy simulations (LES) of isotropic turbulence with a mean scalar gradient. Bos et al. (2004) further suggested that the velocity-scalar cospectrum in the direction of mean scalar gradient can in fact have any slope between $-7/3$ and $-5/3$ based on a cospectral budget analysis. Cava and Katul (2012) showed, using a cospectral budget, that different velocity-scalar scaling laws can be observed in the canopy sublayer above tall forests when the flux transfer term becomes important (Li et al. 2015). Recently, Li and Katul (2017) used a cospectral budget model to show that the $-7/3$ cospectrum scaling can be modified depending on the relative importance of flux transfer and pressure decorrelation terms. These new theoretical developments motivate us to revisit the cospectral scaling in the atmospheric boundary layer (ABL) based on observational data. A specific question to be addressed in this paper is whether the power-law scaling for turbulence cospectra under stable conditions deviates significantly from $-7/3$ at high wavenumbers, and whether it is closer to -2 scaling. As the $-7/3$ scaling was first derived for the stably stratified turbulence by Lumley (1964), here we focus on the stable condition.

2 Dimensional Analysis

According to Kaimal and Finnigan (1994), a cospectrum is the real part of the Fourier transform of cross-covariance. Here we focus on the momentum flux and the sensible heat flux but other scalar fluxes (not shown) such as water vapor and CO_2 are assumed to have the same scaling as the heat flux in the inertial subrange. For sensible heat flux, we have (Kaimal and Finnigan 1994)

$$\langle w'\theta'\rangle = \int_0^\infty E_{w\theta}(k)dk, \tag{1}$$

where $E_{w\theta}$ is the cospectrum of $\langle w'\theta'\rangle$, k the wavenumber, w the vertical velocity, θ the potential temperature, w' the vertical velocity fluctuation, θ' the fluctuation of potential temperature and $\langle\ \rangle$ denotes the Reynolds averaging. Assuming that the cospectrum of heat flux is only related to the gradient of the mean potential temperature $\frac{\partial\Theta}{\partial z}$, the turbulent kinetic energy (TKE) dissipation rate ϵ and the wavenumber k for isotropic turbulence, Lumley (1964) obtained the following form for the cospectrum using dimensional analysis

$$E_{w\theta} = -c_1\epsilon^{1/3}\frac{\partial\Theta}{\partial z}k^{-7/3}, \tag{2}$$

where c_1 is a dimensionless parameter. Similarly, Lumley (1967) suggested cospectrum of the momentum to have the following form:

$$E_{wu} = -c_2\epsilon^{1/3}\frac{\partial U}{\partial z}k^{-7/3}, \tag{3}$$

where c_2 is a dimensionless parameter, u the streamwise velocity and U the mean streamwise velocity.

However, the above dimensional analysis does not yield a unique cospectral scaling law. Assuming that $E_{w\theta}$ is only related to $\frac{g}{\Theta}$ (g is the gravitational acceleration rate), ϵ, $\frac{\partial\Theta}{\partial z}$ and k, based on dimensional analysis, we get:

$$E_{w\theta} = -c_3\left(\frac{g}{\Theta}\frac{\partial\Theta}{\partial z}\right)^{\frac{1-3a}{2}}\epsilon^{a}\frac{\partial\Theta}{\partial z}\ k^{2a-3}, \tag{4}$$

where c_3 and a are dimensionless parameters. When $a=\frac{1}{3}$, this recovers Eq. (2), which is the limit of the Boussinesq approximation where g is absent. When $a=\frac{2}{3}$, this leads to a $-5/3$ scaling, which is the scaling of velocity spectra and is regarded as another limit in

Bos et al. (2004). On the other hand, when $a = \frac{1}{2}$, Eq. (4) yields a -2 power-law scaling for $E_{w\theta}$, as follows:

$$E_{w\theta} = -c_3 \left(\frac{g}{\Theta}\frac{\partial\Theta}{\partial z}\right)^{-1/4} \epsilon^{1/2} \frac{\partial\Theta}{\partial z} k^{-2}. \tag{5}$$

Similarly, assuming that E_{wu} is only related to ϵ, $\frac{\partial U}{\partial z}$ and k, we have (Cava and Katul 2012):

$$E_{wu} = -c_4 \epsilon^{b} \left(\frac{\partial U}{\partial z}\right)^{2-3b} k^{2b-3}, \tag{6}$$

where c_4 and b are dimensionless parameters. Again, when $b = \frac{1}{3}$, this recovers Eq. (3). However, when $b = \frac{1}{2}$, a -2 power-law scaling for E_{wu} emerges, as follows:

$$E_{wu} = -c_4 \epsilon^{1/2} \left(\frac{\partial U}{\partial z}\right)^{1/2} k^{-2}. \tag{7}$$

In summary, a -2 scaling as reported by many previous studies (Mydlarski and Warhaft 1998; Sakai et al. 2008) is also possible based on dimensional analysis.

We emphasize that the above dimensional analysis is only strictly applicable for isotropic turbulence (Kolmogorov 1941). It is generally believed that the Dougherty-Ozmidov scale (Dougherty 1961; Ozmidov 1965) $L_O = 2\pi \left(\frac{\epsilon}{N^3}\right)^{\frac{1}{2}}$ characterizes the largest scale of isotropic turbulence in stably stratified fluid (Gargett et al. 1984; Waite 2011; Grachev et al. 2015; Li et al. 2016), where N is Brunt-Väisälä frequency, which corresponds to the Dougherty-Ozmidov wavenumber $k_O = \frac{2\pi}{L_O}$. Owing to wall effects (Townsend 1976; Katul et al. 2014) in the ASL, the wavenumber $k_a = 1/z$ will also constrain the existence of isotropic turbulence, where z is the height above ground. Therefore, we expect the previously derived power-law scaling for turbulence cospectra to be valid only for wavenumbers $k > \max(k_O, k_a)$.

3 Experiment Setup and Results

3.1 Observations of the stable atmospheric boundary layer

An eddy-covariance (EC) system over Lake Geneva was set up to measure high-frequency (20 Hz) velocity and temperature at 4 different heights (1.66 m, 2.31 m, 2.96 m and 3.61 m above water level) during August-October 2006 (Bou-Zeid et al. 2008). Four sonic anemometers (Campbell Scientific CSAT3) and open-path gas analyzers (LICOR LI-7500) were used in the experiment. The resolution of the wind velocity was 0.001 m s^{-1} and that of temperature was 0.002 ℃. 18 representative 15-minute periods of EC data at 1.66 m were selected to calculate turbulence cospectra of heat and momentum fluxes, where z/L ranged from 0.037 to 0.145 (Table 1), z is the measurement height above water surface, and L is the Obukhov length (Obukhov 1946). The 18 periods ($0.037 \leq \frac{z}{L} \leq 0.145$) in the lake experiment are more stable with larger z/L in 36 available stable periods during August-October 2006 (Bou-Zeid et al. 2008), while the rest datasets (e.g., $\frac{z}{L} \sim 0.01$) are closer to neutral conditions. In the manuscript, we would like to focus on relatively more stable conditions. Besides, the cospectral slopes from all 36 periods (not shown) do not differ from the results from the 18 periods. By estimating the Taylor-microscale-based Reynolds number through $R_\lambda = \left(\frac{20}{3}\frac{q^2}{\epsilon\nu}\right)^{1/2}$, where q is turbulent kinetic energy and ν is kinetic viscosity, as in Pope (2000), we find that R_λ ranged from 657 to 3236 in the 18 periods. The reader is referred to previous studies (Bou-Zeid et al. 2008; Vercauteren et al. 2008; Li and Bou-Zeid 2011; Li et al. 2018) for detailed descriptions of the experiment setup and data.

An EC system at Dome C, Antarctica was set up to measure the high-frequency (10 Hz) velocity and temperature using an ultrasonic anemometer (Metek USA-1) at 3.5 m above ground (Vignon et al. 2017a; Vignon et al. 2017b). Balloon sounding measurements provided temperature gradient (Petenko et al. 2018). The accuracy of wind speed was 0.05 m s^{-1} and that of temperature was 0.01 ℃. 70 representative 30-minute stable periods in 9-12 January 2015 were selected, where z/L ranged from 0.182 to 5.891 (Table 1). The Taylor-microscale-based Reynolds number R_λ ranged from 313 to 2091 in the 70 periods. The reader is referred to Vignon et al. (2017a) for details on the experiment setup.

An EC system over an Arctic ice pack during the Surface Heat Budget of the Arctic Ocean experiment (SHEBA) was set up to measure high-frequency (10 Hz) velocity and temperature using ATI (Applied Technologies, Inc) three-axis sonic anemometer at 2 heights (2.2 m and 3.2 m) from October 1997 through September 1998 (Andreas et al. 2006; Grachev et al. 2013). The resolution of the wind velocity was 0.01 m s^{-1} and that of temperature was 0.01 ℃. 10 representative 60-minute periods of EC data from 8 nights at 3.2 m were selected for analyzing the cospectra of heat and momentum fluxes, where z/L ranged from 0.040 to 2.538 (Table 1). The cospectra were calculated from overlapping 13.65-minute blocks (corresponding to 2^{13} data points) and then averaged over 1-hour periods following (Persson et al. 2002). The experimental setup and data have been extensively discussed elsewhere (Grachev et al. 2005; Andreas et al. 2006; Andreas et al. 2010a; Andreas et al. 2010b; Grachev et al. 2013).

A sonic and hot-film anemometer dyad (Kit et al. 2017) was installed at the Granite Mountain Atmospheric Sciences Testbed (GMAST) of the US army Dugway Proving Ground (DPG), Utah, as part of the field measurements of the Mountain Terrain Atmospheric Modeling and Observations (MATERHORN) program during September-October 2012 (Fernando et al. 2015) to capture fine-scale turbulence in the ABL. Wind velocity was measured at a height of 2 m with a temporal frequency of 2000 Hz. The spatial resolution of the composite probe was ~0.7 mm, and the measurement resolution of the hot-film X-wire probes was ~1mm. 6 representative 30-minute periods on 9 October 2012 were selected for analyzing the momentum cospectrum, where z/L ranged from 0.027 to 0.647 (Table 1). The reader is referred to details on the instrument setup and measurement methods elsewhere (Fernando et al. 2015; Kit and Liberzon 2016; Kit et al. 2017; Sukoriansky et al. 2018).

Table 1 Details of selected stable periods in field observations: eddy-covariance (EC) systems over Lake Geneva, EC systems at Dome C in Antarctica, EC systems of SHEBA campaign in Arctic, and sonic and hot-film anemometer dyad of MATERHORN campaign in Utah. R_λ is the Taylor-microscale-based Reynolds number, u_* is the friction velocity, T_* is the scaling temperature, z is the measurement height above the surface, L is the Obukhov length, w is vertical velocity, T is air temperature, E_{wT} is the cospectrum of $\langle w'T' \rangle$ and E_{wu} is the cospectrum of $\langle w'u' \rangle$. The "mean slope" is the average of fitted slope for cospectrum at high frequencies in the selected periods of field observations, and the corresponding standard deviation is shown in brackets.

Data source	Number of periods	$\boldsymbol{R_\lambda}$	$\boldsymbol{u_*}$ (m s^{-1})	$\boldsymbol{T_*}$ (K)	$\boldsymbol{z/L}$	Mean slope of $\boldsymbol{E_{wT}}$ (standard deviation)	Frequency domain (Hz) of $\boldsymbol{E_{wT}}$	Mean slope of $\boldsymbol{E_{wu}}$ (standard deviation)	Frequency domain (Hz) of $\boldsymbol{E_{wu}}$
Lake Geneva	18	657~3236	0.066~0.167	0.023~0.095	0.037~0.145	-2.02 (0.22)	1.6~3.4	-2.00 (0.85)	0.75~2.0
Dome C	70	313~2091	0.030~0.143	0.014~0.152	0.182~5.891	-2.07 (0.25)	1.4~4.0	-2.11 (0.37)	1.1~2.8
SHEBA	10	-	0.046~0.166	0.033~0.111	0.040~2.538	-1.93 (0.41)	2.0~4.0	-1.99 (0.34)	0.35~1.0
MATERHORN	6	-	0.028~0.176	0.018~0.143	0.027~0.647	-	-	-2.02 (0.12)	5~300

3.2 Turbulence Cospectra

The stability parameter z/L was calculated to characterize the stability of the ABL, where z is the measurement height above the surface, $L = -\frac{u_*^3}{\frac{\kappa g}{\theta_0}\langle w'\theta' \rangle}$ the Obukhov length (Obukhov 1946), u_* the friction velocity, κ the von Kármán constant, θ_0 the mean potential temperature and θ' the fluctuation. Note that we use air temperature to approximate potential temperature as our measurements were all below 3.5 m above the surface. Rather than directly measuring the cospectra in wavenumber space, we converted the frequency cospectra into wavenumber cospectra, invoking Taylor's frozen turbulence hypothesis (Taylor 1938). Wavelet transform (Torrence and Compo 1998) was used to calculate turbulence cospectra (software was provided by C. Torrence and G. Compo, and is available at: http://paos.colorado.edu/research/wavelets/) for observations at Lake Geneva and Dome C. The fast Fourier transform (Frigo and Johnson 1998) was used to calculate turbulence cospectra for observations of the SHEBA and MATERHORN experiments. Both wavelet and Fourier transform are used in this study to eliminate possible effects of the cospectra calculation method on cospectral slopes, while both methods were routinely applied in calculating turbulence cospectra in the ABL (Hudgins et al. 1993; Cornish et al. 2006; Li et al. 2015).

Both frequency and cospectra (based on wavelets) were normalized in a similar way to Kaimal et al. (1972). Four examples from the lake experiment are shown in Fig. 1. A few cospectra at the highest wavenumbers are seen due to the limitation of the instrument temporal sampling. At low wavenumbers, the cospectral slope is shallower than -2, and even approaches zero in some cases (Fig. 1). This is because internal gravity waves (Lumley 1964; Caughey and Readings 1975; Smedman 1988) and wall effects (Townsend 1976; Katul et al. 2014) have stronger impacts on larger eddies. Hence turbulence deviates more from isotropic condition at lower wavenumbers (Lienhard and Van Atta 1990), as expected.

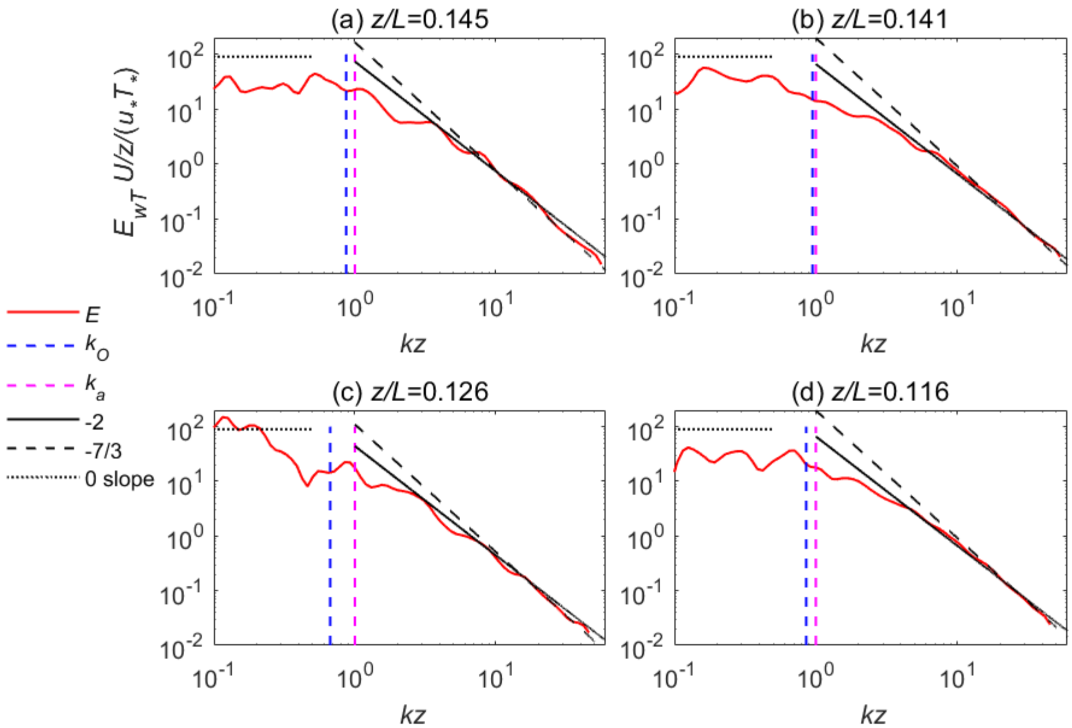

Fig.1 (**a**)~(**d**): Normalized cospectrum of the heat flux in 4 representative 15-minute periods of EC measurements over Lake Geneva. E_{wT} is the wavelet cospectrum of the vertical velocity fluctuations w' and temperature fluctuation T' in time, U the mean streamwise wind velocity, z the measurement height above the lake, u_* the friction velocity, T_* the scaling temperature, k the wavenumber, and L the Obukhov length. E denotes the normalized heat flux cospectrum. k_O and k_a denote the Dougherty-Ozmidov wavenumber and the wavenumber k_a for the distance to the wall, respectively. Note that the units in y axis are not necessarily non-dimensional.

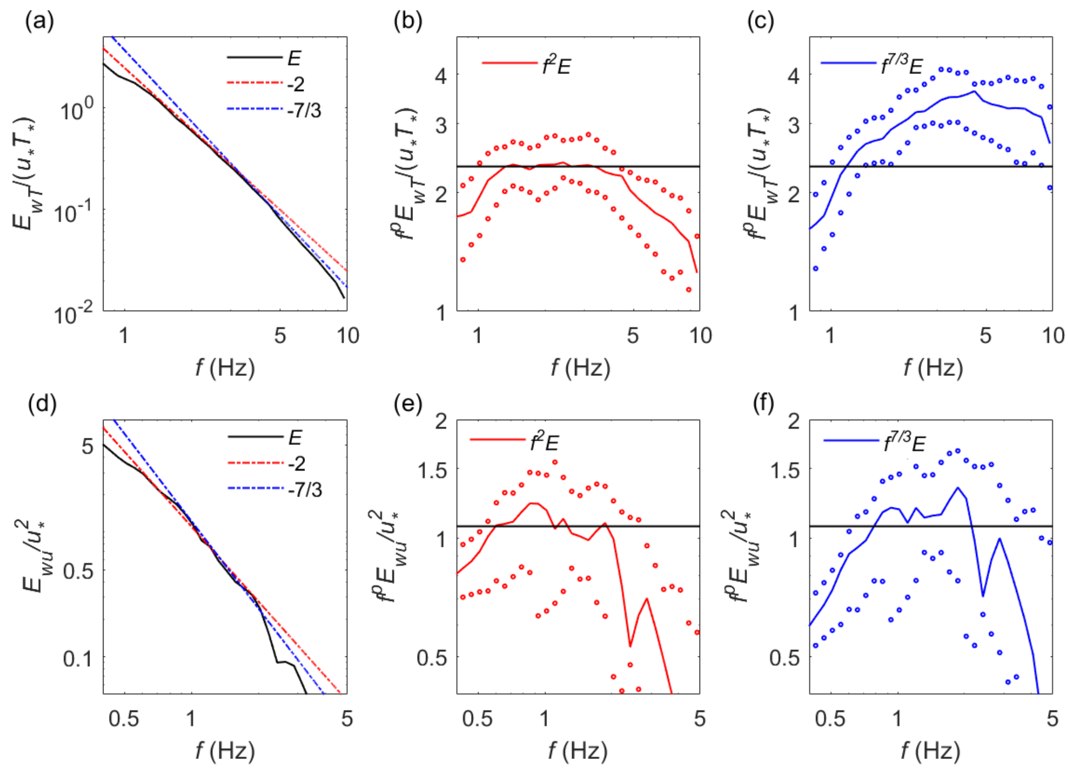

Fig. 2 (**a**) The median of the normalized cospectrum of heat flux (denoted by $E_{wT}/(u_*T_*)$ or E) across 18 representative 15-minute periods over Lake Geneva. (**b**) $E_{wT}/(u_*T_*)$ in (**a**) multiplied by f^2. (**c**) $E_{wT}/(u_*T_*)$ in (**a**) multiplied by $f^{7/3}$. (**d**) The median of normalized cospectrum of momentum flux (denoted by E_{wu}/u_*^2 or E). (**e**) E_{wu}/u_*^2 in (**d**) multiplied by f^2. (**f**) E_{wu}/u_*^2 in (**d**) multiplied by $f^{7/3}$. Empty circles (blue for $f^{7/3}E$ and red for f^2E) denote the 25th and 75th percentiles of cospectrum at each frequency. p is an exponent equal to $7/3$ or 2, f is the sampling frequency in Hz, and the other variables have the same meaning as those in Fig 1.

To further examine whether the -2 or the $-7/3$ slope better captures the observed cospectral scaling at high wavenumbers, the median cospectrum of 18 different stable periods for each frequency is shown (Fig. 2a) for the lake experiment. The -2 slope starts matching the cospectrum at around 1.5 Hz, which is lower compared to that of the $-7/3$ slope. The $-7/3$ slope seems to match the cospectrum at frequencies higher than 5 Hz. In fact, the slope at frequencies higher than 5 Hz is even steeper than $-7/3$. However, Bos et al. (2004) showed that the asymptotic slope should be between $-5/3$ and $-7/3$ using a cospectral budget analysis, and thus a slope steeper than $-7/3$ is likely caused by instrument temporal sampling cutoff.

To better assess the exact slope, we then evaluate the compensated cospectra and multiply the median cospectra by f^2 and $f^{7/3}$, respectively (Fig. 2b and Fig. 2c), where f is the sampling frequency in Hz, to better distinguish the two slopes. At frequencies 1.5

Hz $< f < 4$ Hz, there is a plateau for $f^2 E_{wT}$. However, there is a positive slope before approximately 4.5 Hz and a negative slope after 4.5 Hz for $f^{7/3} E_{wT}$. It is possible that $f^{7/3} E_{wT}$ might reach a plateau at higher frequencies but this cannot be observed due to the instrument sampling cutoff. Besides, the 25th and 75th percentiles of cospectrum denoted by empty circles at each frequency also show a larger plateau in $f^2 E$ compared to $f^{7/3} E$. In Dome C observations, it is harder to observe a plateau for $f^{7/3} E_{wT}$ but a small plateau exists for $f^2 E_{wT}$ at around 2 Hz (Fig. 3a and Fig. 3b) for the heat flux. In the SHEBA campaign, the median of $f^{7/3} E_{wT}$ shows a positive slope from 2 to 4 Hz but $f^2 E_{wT}$ has a plateau in the same frequency regime (Fig. 4a and Fig. 4b). The cospectrum jump after 4 Hz is possibly due to instrumental noise. These atmospheric observations of the compensated cospectra therefore suggest that -2 better characterizes the cospectral scaling of sensible heat flux at high frequencies (> 2 Hz) compared to $-7/3$.

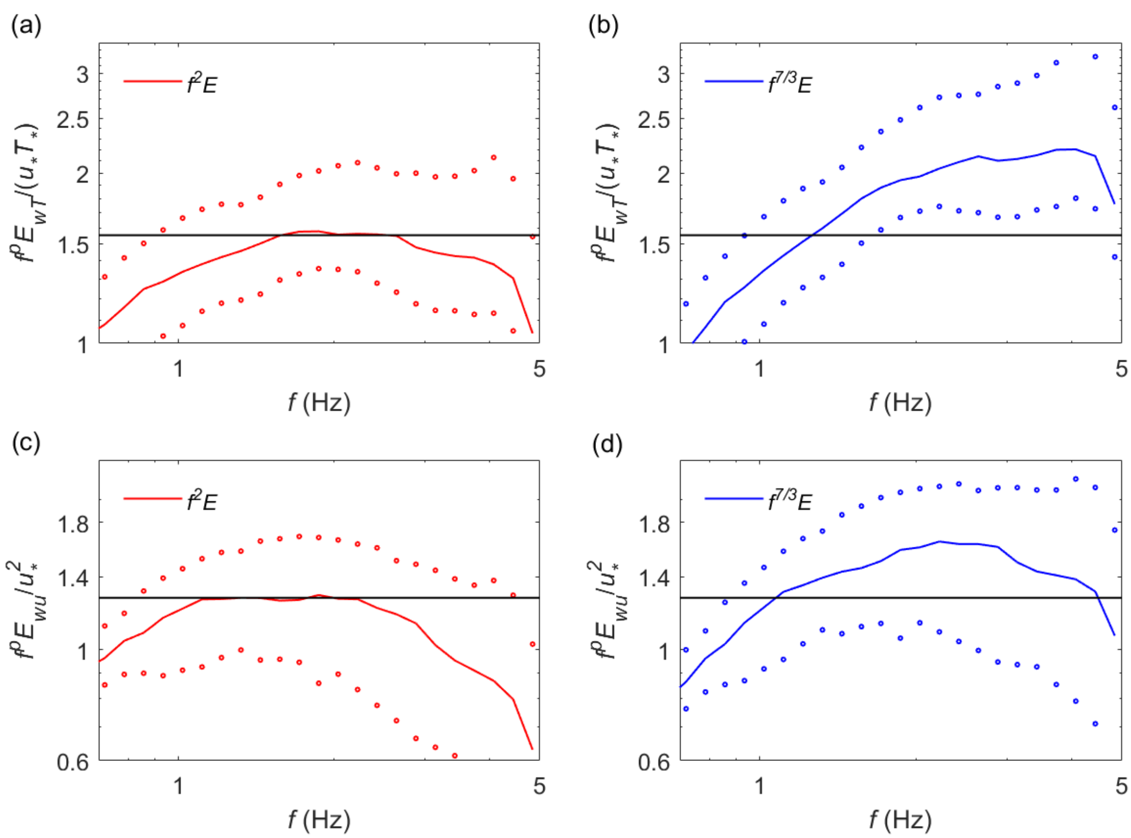

Fig. 3 The median of normalized cospectra of (**a**) heat flux (denoted by $E_{wT}/(u_* T_*)$ or E) multiplied by f^2 (**b**) heat flux (denoted by $E_{wT}/(u_* T_*)$ or E) multiplied by $f^{7/3}$ (**c**) momentum flux (denoted by E_{wu}/u_*^2 or E) multiplied by or f^2 (**d**) momentum flux (denoted by E_{wu}/u_*^2 or E) multiplied by or $f^{7/3}$ across 70 representative 30-minute periods at Dome C. Empty circles (blue for $f^{7/3} E$ and red for $f^2 E$) denote the 25th and 75th percentiles of cospectrum at each frequency. p is an exponent equal to $7/3$ or 2, f is the sampling frequency in Hz, and the other variables have the same meaning as those in Fig. 1.

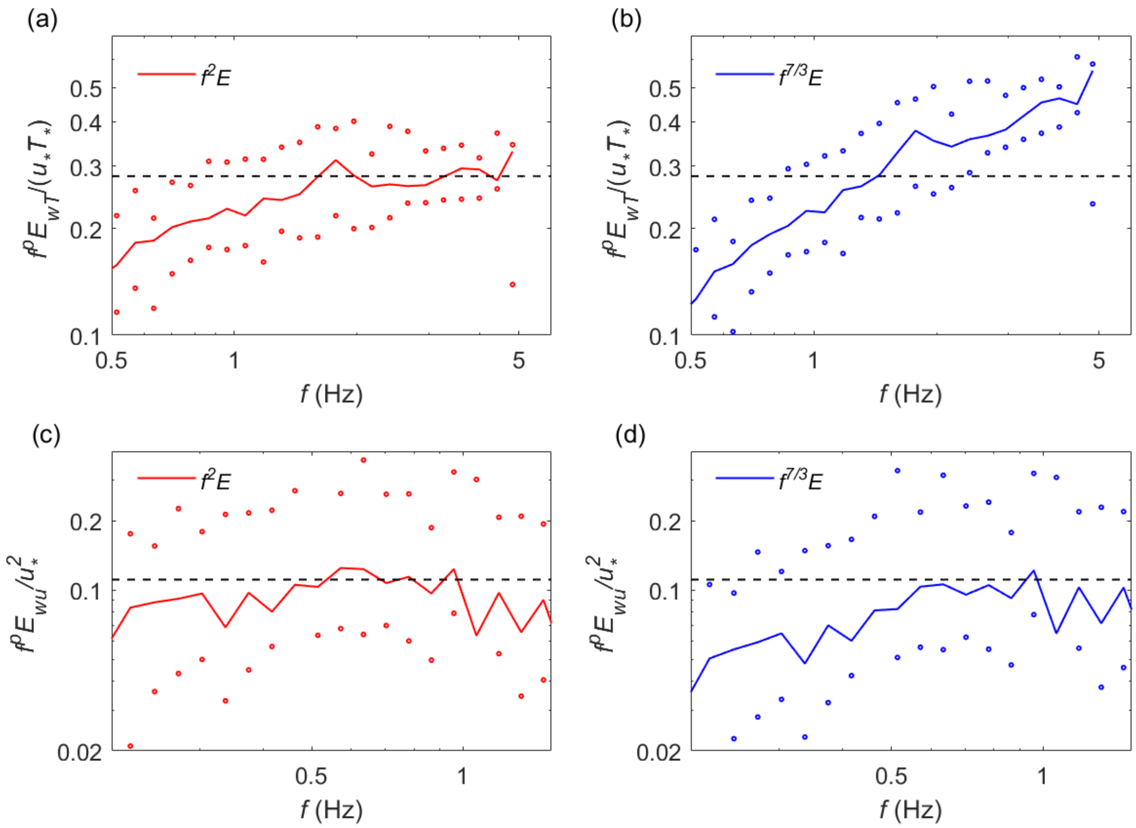

Fig. 4 The median of normalized cospectra of (**a**) heat flux (denoted by $E_{wT}/(u_*T_*)$ or E) multiplied by f^2 (**b**) heat flux (denoted by $E_{wT}/(u_*T_*)$ or E) multiplied by $f^{7/3}$ (**c**) momentum flux (denoted by E_{wu}/u_*^2 or E) multiplied by or f^2 (**d**) momentum flux (denoted by E_{wu}/u_*^2 or E) multiplied by or $f^{7/3}$ across 10 representative averaged 13.65-minute periods from the SHEBA experiment. Empty circles (blue for $f^{7/3}E$ and red for f^2E) denote the 25th and 75th percentiles of cospectrum at each frequency. p is an exponent equal to 7/3 or 2, f is sampling frequency in Hz and the other variables have the same meaning as those in Fig. 1.

For the momentum flux cospectrum (Fig. 2d, Fig. 2e and Fig. 2f), the difference between the -2 and $-7/3$ slopes is smaller than that of heat flux cospectrum in the lake experiment. In the Dome C observation, a plateau is observed for f^2E_{wu} at 1.5~2.5 Hz (Fig. 3c) but not for $f^{7/3}E_{wu}$ (Fig. 3d), which keeps increasing with frequency. In the SHEBA campaign, a slightly larger plateau is seen in f^2E_{wu} compared to $f^{7/3}E_{wu}$ in high-frequency parts (Fig. 4c and Fig. 4d). In the MATERHORN campaign, the median of $f^{7/3}E_{wu}$ shows a positive slope from 10 Hz to 300 Hz while f^2E_{wu} is flat in the same frequency regime (Fig. 5). Again, the cospectral scaling of momentum flux better matches -2 than $-7/3$ in these field observations.

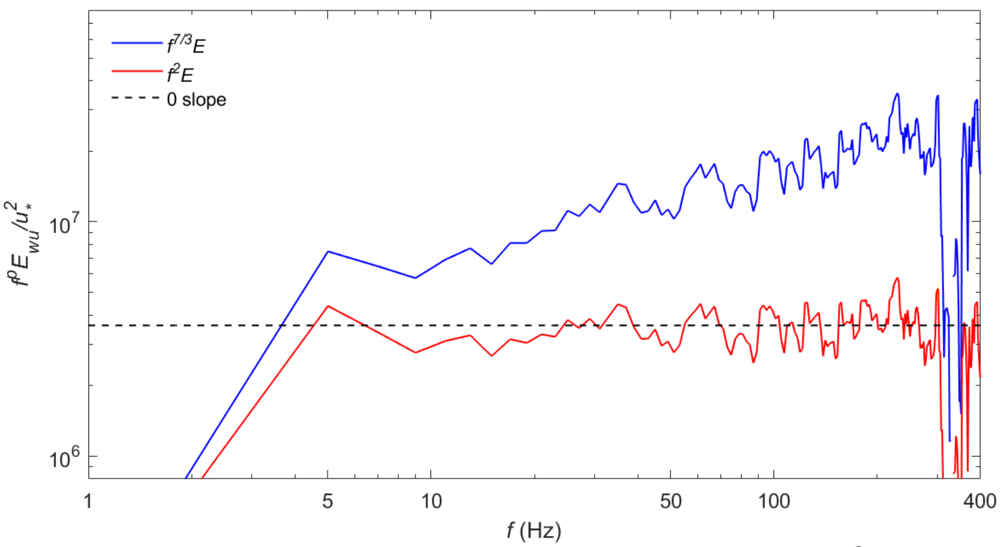

Fig. 5 The median of normalized cospectrum of momentum flux (denoted by E_{wu}/u_*^2 or E) multiplied by $f^{7/3}$ (blue lines) or f^2 (red lines) across 6 representative 30-minute periods from the MATERHORN experiment. p is an exponent equal to 7/3 or 2 and f is the sampling frequency in Hz and other variables have the same meaning as those in Fig. 1.

In addition to these analyses, we further fitted a slope for the heat flux cospectrum between 1.6 Hz and 3.4 Hz in each period (e.g., the frequency domain in Fig. 2b) and obtained a mean slope of -2.03 and a standard deviation of 0.22 for 18 periods (Table 1) in the lake experiment. The frequency domain was selected to ensure that the cospectrum started to match a power-law at the lower limit and was not influenced by instrumental cutoff at the higher limit. We extended the frequency range by 33.3%, within 1.3 Hz $< f <$ 3.7 Hz, and found a slope of -2.02, which is very close to the initial -2.03 slope estimate. We performed similar sensitivity test of the slope fitting the slopes of the cospectra in other datasets. The fitted slope for the heat flux cospectra in the Dome C and SHEBA campaigns are -2.07 and -1.93, with a standard deviation of 0.25 and 0.41, respectively (Table 1). Therefore, based on our data, a -2 scaling appears to be more likely observed than the $-7/3$ (-2.33) cospectrum for the heat flux. For the cospectrum of momentum flux, the fitted slope in the 4 campaigns are -2.00, -2.11, -1.99 and -2.02, respectively (Table 1), again close to a -2 slope. It is worth noting that the standard deviation of the momentum cospectra is generally larger than that of heat cospectra (Table 1), which is consistent with the larger ratio of the 25th to 75th percentiles of cospectrum in momentum flux (Fig. 2b and Fig. 2e) due to the more variable nature of momentum compared to scalars.

A $-7/3$ power-law scaling would indicate that $E_{wT} \propto \epsilon^{1/3}$ according to Eq. (2), while a -2 power-law scaling would suggest that $E_{wT} \propto \epsilon^{1/2}$ according to Eq. (5). Similarly, a $-7/3$ scaling would indicate that $E_{wu} \propto \epsilon^{1/3}$ according to Eq. (3), while a -2 scaling would suggest that $E_{wu} \propto \epsilon^{1/2}$ according to Eq. (7). It is thus helpful to examine the power-law relation of E_{wT} (E_{wu}) with ϵ to further determine the cospectra slope. We fitted a linear relationship between normalized E_{wT} and $\epsilon^{1/3}$ in a log-log plot (Fig. 6a) for the 18 periods of observations (minimizing the sum of squared errors) in the lake experiment and obtained a coefficient of determination $R^2 = 0.55$. We also fitted a linear relationship between normalized E_{wT} and $\epsilon^{1/2}$ in the log-log plot (Fig. 6b) and obtained $R^2 = 0.73$, suggesting that $E_{wT} \propto \epsilon^{1/2}$ is a better approximation and thus further confirming that the -2 scaling better captures the heat flux cospectrum. In addition, we fitted a linear regression between normalized E_{wu} and ϵ in a similar way as Fig. 6a and obtained $R^2 = 0.56$ (see Fig. 7a). We fitted a linear regression between the normalized E_{wu} and ϵ in a way similar to Fig. 6b and obtained $R^2 = 0.74$ (see Fig. 7b). This also suggests that $E_{wu} \propto \epsilon^{1/2}$ is a better approximation, and thus -2 scaling better captures the momentum flux cospectrum than the $-7/3$ scaling.

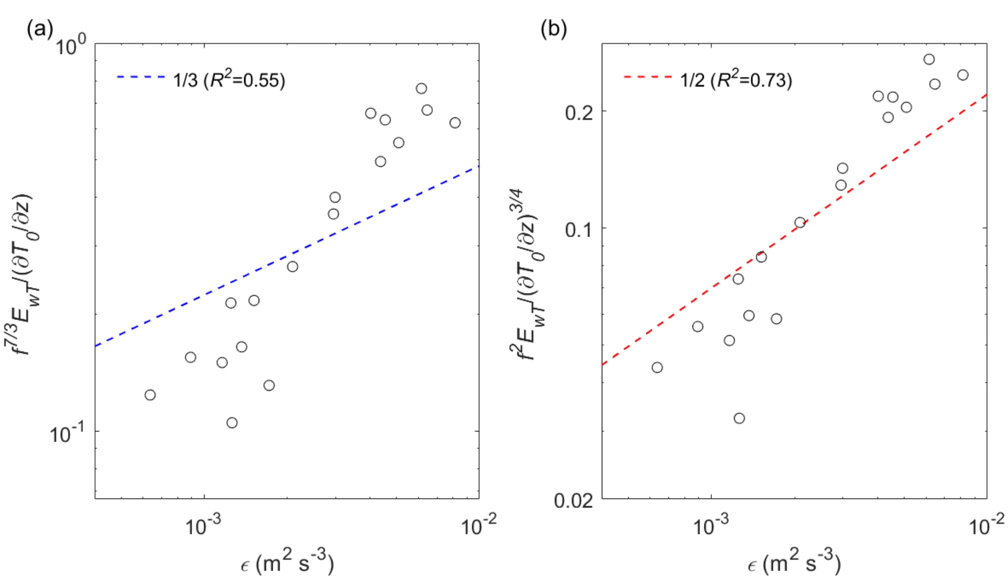

Fig. 6 Normalized cospectrum of heat flux plotted against the mean turbulent kinetic energy dissipation rate (ϵ) in 18 representative 15-minute periods collected over Lake Geneva. (**a**) $f^{7/3}E_{wT}\left(\frac{\partial T_0}{\partial z}\right)^{-1}$ according to Eq.

(2). (**b**) $f^2 E_{wT}\left(\frac{\partial T_0}{\partial z}\right)^{-3/4}$ according to Eq. (5). T_0 is mean temperature in time, ϵ is mean turbulent energy dissipation rate, R^2 is the coefficient of determination and the other variables have the same meaning as those in Fig. 1.

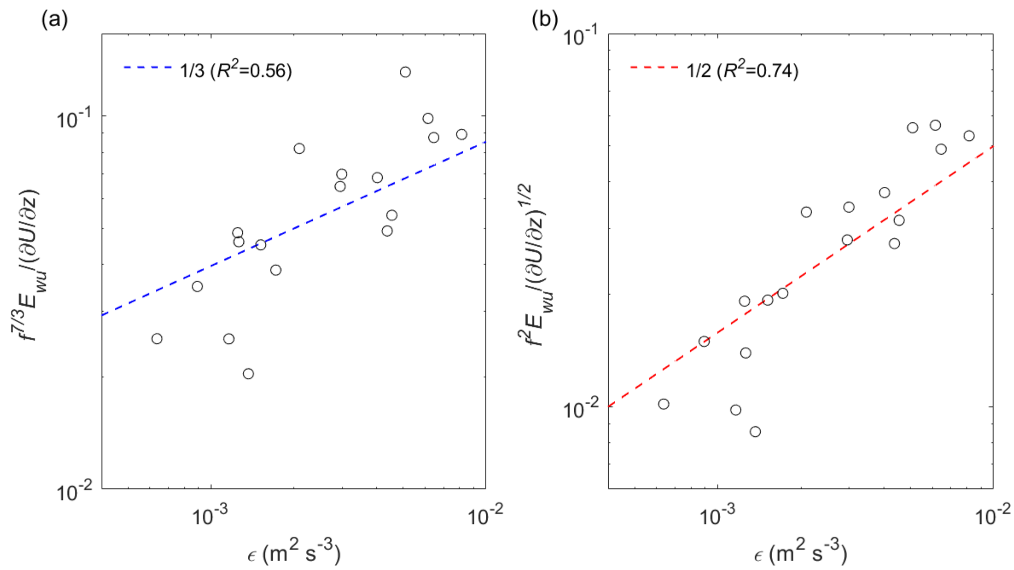

Fig. 7 Normalized cospectrum of momentum flux plotted against the mean turbulent kinetic energy dissipation rate (ϵ) in 18 representative 15-minute periods collected over Lake Geneva. (**a**) $f^{7/3}E_{wu}\left(\frac{\partial U}{\partial z}\right)^{-1}$ according to Eq. (3). (**b**) $f^2 E_{wu}\left(\frac{\partial U}{\partial z}\right)^{-1/2}$ according to Eq. (7). R^2 is the coefficient of determination and the other variables have the same meaning as those in Fig. 1.

To further conclude our analysis, we examine the "structure function" of the temperature flux (Mydlarski 2003),

$$D_{wT} = \langle \Delta w \Delta T \rangle, \tag{8}$$

where $\Delta w \equiv w(x+r) - w(x)$, $\Delta T \equiv T(x+r) - T(x)$, x is spatial coordinate and r is the spatial separation between two points. We also defined the higher-order functions $D_{w^2T^2} = \langle (\Delta w \Delta T)^2 \rangle$ and $D_{w^4T^4} = \langle (\Delta w \Delta T)^4 \rangle$. Similarly, $D_{wu} = \langle \Delta w \Delta u \rangle$ denotes the structure function of momentum flux, and $D_{w^2u^2} = \langle (\Delta w \Delta u)^2 \rangle$ and $D_{w^4u^4} = \langle (\Delta w \Delta u)^4 \rangle$. Following Antonia and Van Atta (1978), the temporal measurements were used to represent the spatial structure functions by invoking Taylor's frozen turbulence hypothesis (Taylor 1938). The $-7/3$ scaling of cospectrum would indicate $D_{wT} \propto r^{4/3}$ ($D_{w^2T^2} \propto r^{8/3}$ and $D_{w^4T^4} \propto r^{16/3}$ respectively) in the inertial subrange (Mydlarski 2003), while the -2 scaling would indicate $D_{wT} \propto r$ ($D_{w^2T^2} \propto r^2$ and $D_{w^4T^4} \propto r^4$ respectively). The structure function D_{wT} is therefore multiplied by $r^{-4/3}$ and r^{-1}, respectively (Fig. 8a), for the lake data. At scales smaller than 0.5 m, $r^{-1}D_{wT}$ exhibits a plateau, while $r^{-4/3}D_{wT}$ has a steeper, positive, slope (Fig. 8a). For the momentum structure function, a flat region for $r^{-1}D_{wu}$ at 0.7 m $< r <$ 1.5 m can be observed, while there is only a much smaller plateau for $r^{-4/3}D_{wu}$ (Fig. 8b). The flat region of $r^{-1}D_{wT}$ ($r^{-1}D_{wu}$) corresponds to the relation $D_{wT} \propto r$ ($D_{wu} \propto r$) and a -2 scaling of the cospectrum. The abrupt change of slope at $r <$ 0.3 m for the compensated D_{wT} (Fig. 8a) and at $r <$ 0.6 m for the compensated D_{wu} (Fig. 8b) suggests smaller amplitude of D_{wT} and D_{wu}, which could be due to relatively larger instrument noise at small spatial separation. This noise effect is reduced for even-order functions, such as $D_{w^2T^2}$ (Fig. 8c) and $D_{w^4T^4}$ (Fig. 8e) since they are more stable. The normalized higher-order functions $r^{-2}D_{w^2T^2}$, $r^{-2}D_{w^2u^2}$, and $r^{-4}D_{w^4T^4}$ and $r^{-4}D_{w^4u^4}$ thus approach a plateau at the smallest scales (Figs. 8c, 8d, 8e & 8f), while there is still an obvious negative slope at the smallest scales for $r^{-8/3}D_{w^2T^2}$, $r^{-8/3}D_{w^2u^2}$, $r^{-16/3}D_{w^4T^4}$ and $r^{-16/3}D_{w^4u^4}$. These results suggest that the relationships $D_{w^2T^2} \propto r^2$ and $D_{w^4T^4} \propto r^4$ are better approximations of the structure functions. Similar results are seen at the Dome C observations (Fig. 9). It is worth noting that the plateau occurs at larger scales (i.e., a larger inertial subrange) for low-order functions $r^{-1}D_{wT}$ and $r^{-1}D_{wu}$ than higher-order functions $r^{-2}D_{w^2T^2}$, $r^{-2}D_{w^2u^2}$, and $r^{-4}D_{w^4T^4}$ and $r^{-4}D_{w^4u^4}$, which is consistent with the finding that higher-order structure functions (Kolmogorov 1941) produce narrower inertial subrange (Van Atta and Chen 1970; Anselmet et al. 1984). Therefore, the structure functions of the fluxes suggest that the -2 scaling is a better approximation for turbulence cospectra than $-7/3$ scaling across a wide range of observed stable conditions.

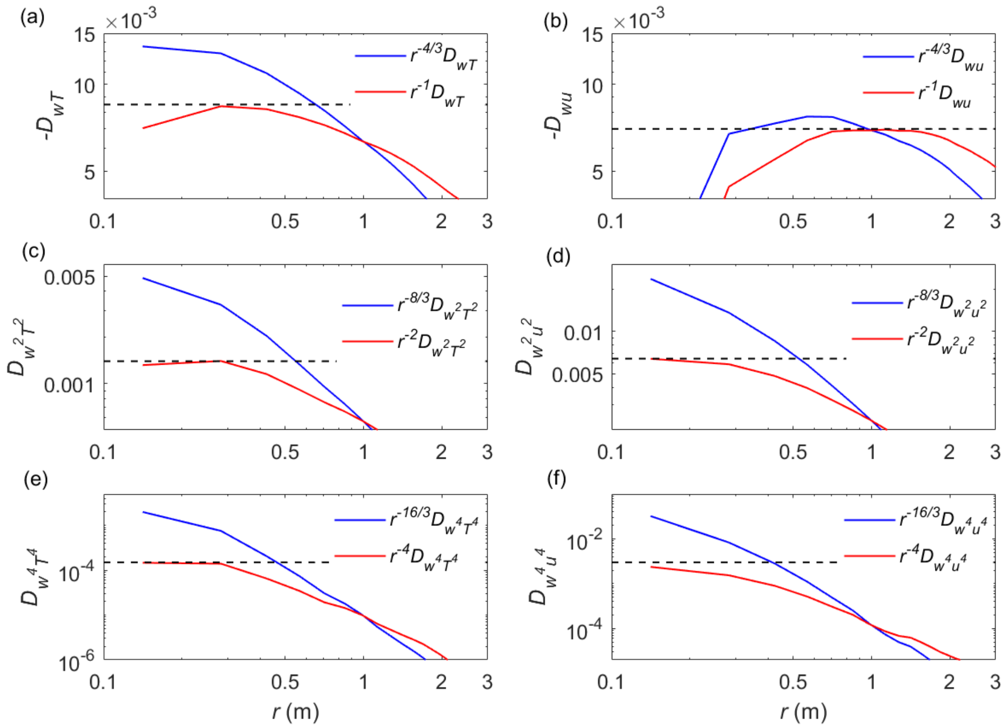

Fig. 8 The median of normalized structure function of (**a**) D_{wT} (**b**) D_{wu} (**c**) $D_{w^2T^2}$, (**d**) $D_{w^2u^2}$, (**e**) $D_{w^4T^4}$ and (**f**) $D_{w^4T^4}$ across 18 representative 15-minute periods over Lake Geneva. r is the spatial separation.

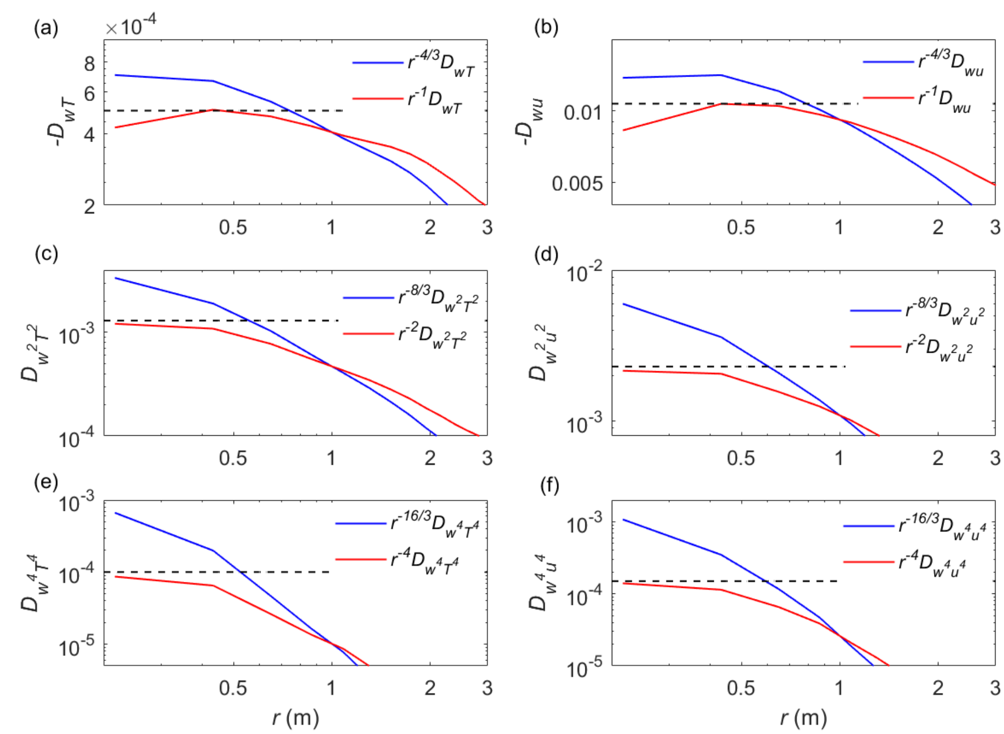

Fig. 9 The median of normalized structure function of (**a**) D_{wT} (**b**) D_{wu} (**c**) $D_{w^2T^2}$, (**d**) $D_{w^2u^2}$, (**e**) $D_{w^4T^4}$ and (**f**) $D_{w^4T^4}$ across 70 representative 30-minute periods at Dome C.

3.3 Discussion

Our field observations (with the highest Taylor-microscale-based Reynolds number of $R_\lambda = 3236$) are consistent with previous laboratory experiments (Mydlarski and Warhaft 1998; Mydlarski 2003; Sakai et al. 2008), which reported a -2 spectral scaling for turbulence cospectra at Taylor-microscale-based Reynolds number below 582. Previous numerical simulations (Bos et al. 2004; O'Gorman and Pullin 2005) also showed a -2 scaling in homogeneous and isotropic turbulence with a mean scalar gradient. It is worth noting that some studies (Kaimal et al. 1972; Saddoughi and Veeravalli 1994; Bos 2014) suggested a $-7/3$ scaling for the cospectra but did not compare their results with other scaling exponents, in particular to the -2 scaling proposed here. Therefore, it is reasonable to infer that $-7/3$ scaling has not been firmly established as the proper scaling for cospectra of heat, momentum and scalar fluxes at moderate Reynolds numbers ($R_\lambda \sim 10^3$).

In terms of theoretical analyses, O'Gorman and Pullin (2003) proposed that both a $-5/3$ scaling leading term and a next-order $-7/3$ scaling term contribute to the cospectrum of velocity and scalar based on a stretched-spiral vortex model. Bos et al. (2005) showed using eddy-damped quasi-normal Markovian (EDQNM) (Orszag 1970) closure that the $-7/3$ scaling for velocity-scalar cospectrum could only be observed at very high Taylor-microscale Reynolds number ($R_\lambda = 10^7$) while a smaller cospectral scaling exponent could be observed at lower Reynolds numbers. Li and Katul (2017) showed that deviations from $-7/3$ are related to the flux transfer and pressure decorrelation terms for momentum flux budget, while the exact value of the scaling cannot be determined from this model. In other words, these theoretical models imply the possibility of -2 scaling at moderate Reynolds numbers ($R_\lambda \sim 10^3$) such as in the stable ABL (Bradley et al. 1981; Gulitski et al. 2007). Recent studies (Stiperski and Calaf 2018; Stiperski et al. 2019) suggested that the anisotropy of the Reynolds stress tensor are linked to the turbulence similarity scaling. Although our observations do not demonstrate how the anisotropy of the Reynolds stress tensor directly influences the cospectral scaling, it might still be of interest to explore the effects of the anisotropy in future studies with high-resolution numerical simulations free from measurement errors.

As for the application of the cospectral scaling in spectral corrections of EC observations in the ABL, equation (33) in Kaimal et al. (1972) suggested a -2.1 power-law scaling for the cospectra of heat and momentum fluxes at high wavenumbers, while they suggested $-7/3$ slope as the asymptotic cospectral scaling. The -2.1 slope was then adopted in the spectral correction method by Moore (1986). Yet, Horst (1997) assumed a -2 scaling for scalar cospectrum as it better approximated to his observations, as well as considering the ease of analytical computations. Similarly, Massman (2000) and Massman and Lee (2002) applied a -2 scaling for cospectral correction of EC measurements. Massman (2000) further suggested that the corrections for EC measurements are sensitive to the exact shape of turbulence cospectra in stable conditions. As such, the -2 scaling has already been applied in some earlier spectral correction methods of EC measurements, yet without strong justification. In this paper, we provided evidence from multiple observational field campaigns that the cospectra might follow the -2 spectral scaling in the stable ABL rather than a $-7/3$ scaling typically assumed.

However, there remains open questions. The asymptotic cospectral scaling at infinite Reynolds number is still unknown. The cospectral scaling at $R_\lambda \sim 10^3$ in the stable ABL may not be directly extendable to higher Reynolds numbers, for example $R_\lambda \sim 10^7$ (Bos et al. (2005). While such larger Reynolds numbers are of theoretical interest, our study covers some typical Reynolds numbers of natural stable ABLs and hence of immediate utility.

4 Conclusion

Our field observations in the stable ABL suggest that $-7/3$ may not accurately describe the cospectral scaling when the compensated cospectrum, the relation between cospectrum and turbulent kinetic energy dissipation rate and the "structure function" of fluxes are carefully examined. The observations are consistent with moderate Reynolds number ($R_\lambda \leq 10^3$) results of laboratory experiments (Mydlarski and Warhaft 1998; Mydlarski 2003; Sakai et al. 2008), DNS (O'Gorman and Pullin 2005; Watanabe and Gotoh 2007) and LES (Bos et al. 2004) studies, which compared the -2 power-law scaling with the $-7/3$ power-law scaling. Although whether asymptotic cospectral scaling exists at infinite Reynolds numbers is yet unknown, our observations suggest that -2 might be a better approximation for cospectral scaling for stably stratified ABL at field Reynolds numbers. Therefore, the -2 power-law scaling is recommended for spectral corrections of eddy-covariance measurements in the stable ABL.

Acknowledgements PG would like to acknowledge funding from the National Science Foundation (NSF CAREER, EAR-1552304), and from the Department of Energy (DOE Early Career, DE-SC00142013). The lake data were collected by the Environmental Fluid Mechanics and Hydrology Laboratory of Professor M. Parlange at l'Ecole Polytechnique Fédérale de Lausanne. We would like to thank Prof. M. Parlange and Prof. Elie Bou-Zeid for sharing Lake EC data. Mountain Terrain Atmospheric Modeling and Observations (MATERHORN) program was funded by the Office of Naval Research (N00014-11-1-0709). Dome C data were acquired in the frame of the projects Mass lost in wind flux (MALOX) and Concordia multi-process atmospheric studies (COMPASS) sponsored by PNRA. A special thanks to P. Grigioni and all the staff of Antarctic Meteorological Observatory of Concordia for providing the radio sounding used in this study. And a special thanks to Dr. Igor Petenko of CNR ISAC for running the field experiment at Concordia station.

References

Andreas EL, Claffey KJ, Jordan RE, Fairall CW, Guest PS, Persson POG and Grachev AA (2006) Evaluations of the von Kármán constant in the atmospheric surface layer. Journal of Fluid Mechanics. 559:117-149

Andreas EL, Horst TW, Grachev AA, Persson POG, Fairall CW, Guest PS and Jordan RE (2010a) Parametrizing turbulent exchange over summer sea ice and the marginal ice zone. Quarterly Journal of the Royal Meteorological Society. 136(649):927-943

Andreas EL, Persson POG, Grachev AA, Jordan RE, Horst TW, Guest PS and Fairall CW (2010b) Parameterizing turbulent exchange over sea ice in winter. Journal of Hydrometeorology. 11(1):87-104

Anselmet F, Gagne Y, Hopfinger E and Antonia R (1984) High-order velocity structure functions in turbulent shear flows. Journal of Fluid Mechanics. 140:63-89

Antonia R and Van Atta C (1978) Structure functions of temperature fluctuations in turbulent shear flows. Journal of Fluid Mechanics. 84(3):561-580

Aubinet M, Grelle A, Ibrom A, Rannik Ü, Moncrieff J, Foken T, Kowalski AS, Martin PH, Berbigier P and Bernhofer C (1999) Estimates of the annual net carbon and water exchange of forests: the EUROFLUX methodology. In: Fitter AH and Raffaelli DG (eds.), Advances in Ecological Research, vol 30, Academic Press, pp 113-175

Bos W (2014) On the anisotropy of the turbulent passive scalar in the presence of a mean scalar gradient. Journal of Fluid Mechanics. 744:38-64

Bos W, Touil H and Bertoglio J-P (2005) Reynolds number dependency of the scalar flux spectrum in isotropic turbulence with a uniform scalar gradient. Physics of Fluids. 17(12):125108

Bos W, Touil H, Shao L and Bertoglio J-P (2004) On the behavior of the velocity-scalar cross correlation spectrum in the inertial range. Physics of Fluids. 16(10):3818-3823

Bou-Zeid E, Vercauteren N, Parlange MB and Meneveau C (2008) Scale dependence of subgrid-scale model coefficients: an a priori study. Physics of Fluids. 20(11):115106

Bradley EF, Antonia R and Chambers A (1981) Turbulence Reynolds number and the turbulent kinetic energy balance in the atmospheric surface layer. Boundary-Layer Meteorology. 21(2):183-197

Caughey S and Readings C (1975) An observation of waves and turbulence in the earth's boundary layer. Boundary-Layer Meteorology. 9(3):279-296

Cava D and Katul G (2012) On the scaling laws of the velocity-scalar cospectra in the canopy sublayer above tall forests. Boundary-Layer Meteorology. 145(2):351-367

Cornish CR, Bretherton CS and Percival DB (2006) Maximal overlap wavelet statistical analysis with application to atmospheric turbulence. Boundary-Layer Meteorology. 119(2):339-374

Dougherty J (1961) The anisotropy of turbulence at the meteor level. Journal of Atmospheric and Terrestrial Physics. 21(2-3):210-213

Fernando H, Pardyjak E, Di Sabatino S, Chow F, De Wekker S, Hoch S, Hacker J, Pace J, Pratt T and Pu Z (2015) The MATERHORN: Unraveling the intricacies of mountain weather. Bulletin of the American Meteorological Society. 96(11):1945-1967

Frigo M and Johnson SG (1998) FFTW: An adaptive software architecture for the FFT. Proceedings of the 1998 IEEE International Conference on Acoustics, Speech and Signal Processing, Seattle, WA, USA, 1998, vol 3, IEEE, pp 1381-1384

Gargett A, Osborn T and Nasmyth P (1984) Local isotropy and the decay of turbulence in a stratified fluid. Journal of Fluid Mechanics. 144:231-280

Grachev AA, Andreas EL, Fairall CW, Guest PS and Persson POG (2013) The critical Richardson number and limits of applicability of local similarity theory in the stable boundary layer. Boundary-Layer Meteorology. 147(1):51-82

Grachev AA, Andreas EL, Fairall CW, Guest PS and Persson POG (2015) Similarity theory based on the Dougherty–Ozmidov length scale. Quarterly Journal of the Royal Meteorological Society. 141(690):1845-1856

Grachev AA, Fairall CW, Persson POG, Andreas EL and Guest PS (2005) Stable boundary-layer scaling regimes: the SHEBA data. Boundary-Layer Meteorology. 116(2):201-235

Gulitski G, Kholmyansky M, Kinzelbach W, Lüthi B, Tsinober A and Yorish S (2007) Velocity and temperature derivatives in high-Reynolds-number turbulent flows in the atmospheric surface layer. Part 1. Facilities, methods and some general results. Journal of Fluid Mechanics. 589:57-81

Horst T (1997) A simple formula for attenuation of eddy fluxes measured with first-order-response scalar sensors. Boundary-Layer Meteorology. 82(2):219-233

Hudgins L, Friehe CA and Mayer ME (1993) Wavelet transforms and atmopsheric turbulence. Physical Review Letters. 71(20):3279

Kaimal JC and Finnigan JJ (1994) Atmospheric boundary layer flows: their structure and measurement. Oxford University Press, New York, 289 pp

Kaimal JC, Wyngaard JC, Izumi Y and Cote OR (1972) Spectral characteristics of surface-layer turbulence. Quarterly Journal of the Royal Meteorological Society. 98(417):563-589

Katul GG, Porporato A, Shah S and Bou-Zeid E (2014) Two phenomenological constants explain similarity laws in stably stratified turbulence. Physical Review E. 89(2):023007

Kit E, Hocut C, Liberzon D and Fernando H (2017) Fine-scale turbulent bursts in stable atmospheric boundary layer in complex terrain. Journal of Fluid Mechanics. 833:745-772

Kit E and Liberzon D (2016) 3D-calibration of three-and four-sensor hot-film probes based on collocated sonic using neural networks. Measurement Science and Technology. 27(9):095901

Kolmogorov AN (1941) The local structure of turbulence in incompressible viscous fluid for very large Reynolds numbers. Dokl. Akad. Nauk SSSR, 1941, vol 30, pp 299-303

Kovasznay LS (1948) Spectrum of locally isotropic turbulence. Journal of the Aeronautical Sciences. 15(12):745-753

Leuning R and Moncrieff J (1990) Eddy-covariance CO2 flux measurements using open-and closed-path CO2 analysers: corrections for analyser water vapour sensitivity and damping of fluctuations in air sampling tubes. Boundary-Layer Meteorology. 53(1-2):63-76

Li D and Bou-Zeid E (2011) Coherent structures and the dissimilarity of turbulent transport of momentum and scalars in the unstable atmospheric surface layer. Boundary-Layer Meteorology. 140(2):243-262

Li D and Katul GG (2017) On the linkage between the k−5/3 spectral and k−7/3 cospectral scaling in high-Reynolds number turbulent boundary layers. Physics of Fluids. 29(6):065108

Li D, Katul GG and Bou-Zeid E (2015) Turbulent energy spectra and cospectra of momentum and heat fluxes in the stable atmospheric surface layer. Boundary-Layer Meteorology. 157(1):1-21

Li D, Salesky ST and Banerjee T (2016) Connections between the Ozmidov scale and mean velocity profile in stably stratified atmospheric surface layers. Journal of Fluid Mechanics. 797:R3

Li Q, Bou-Zeid E, Vercauteren N and Parlange M (2018) Signatures of Air–Wave Interactions Over a Large Lake. Boundary-Layer Meteorology. 167(3):445-468

Lienhard JH and Van Atta CW (1990) The decay of turbulence in thermally stratified flow. Journal of Fluid Mechanics. 210:57-112

Lumley JL (1964) The spectrum of nearly inertial turbulence in a stably stratified fluid. Journal of the Atmospheric Sciences. 21(1):99-102

Lumley JL (1967) Theoretical aspects of research on turbulence in stratified flows. Proc. Int. Colloquium Atmospheric Turbulence and Radio Wave Propagation, 1967, pp 105-110

Mamadou O, de la Motte LG, De Ligne A, Heinesch B and Aubinet M (2016) Sensitivity of the annual net ecosystem exchange to the cospectral model used for high frequency loss corrections at a grazed grassland site. Agricultural and Forest Meteorology. 228:360-369

Massman WJ (2000) A simple method for estimating frequency response corrections for eddy covariance systems. Agricultural and Forest Meteorology. 104(3):185-198

Massman WJ and Lee X (2002) Eddy covariance flux corrections and uncertainties in long-term studies of carbon and energy exchanges. Agricultural and Forest Meteorology. 113(1):121-144

Moncrieff JB, Massheder J, De Bruin H, Elbers J, Friborg T, Heusinkveld B, Kabat P, Scott S, Søgaard H and Verhoef A (1997) A system to measure surface fluxes of momentum, sensible heat, water vapour and carbon dioxide. Journal of Hydrology. 188:589-611

Monin A and Yaglom A (1975) Statistical fluid mechanics: mechanics of turbulence. MIT Press, Cambridge, Massachusetts, 874 pp

Moore C (1986) Frequency response corrections for eddy correlation systems. Boundary-Layer Meteorology. 37(1-2):17-35

Mydlarski L (2003) Mixed velocity–passive scalar statistics in high-Reynolds-number turbulence. Journal of Fluid Mechanics. 475:173-203

Mydlarski L and Warhaft Z (1998) Passive scalar statistics in high-Péclet-number grid turbulence. Journal of Fluid Mechanics. 358:135-175

O'Gorman P and Pullin D (2005) Effect of Schmidt number on the velocity–scalar cospectrum in isotropic turbulence with a mean scalar gradient. Journal of Fluid Mechanics. 532:111-140

O’Gorman P and Pullin D (2003) The velocity-scalar cross spectrum of stretched spiral vortices. Physics of Fluids. 15(2):280-291

Obukhov A (1946) Turbulence in thermally inhomogeneous atmosphere. Trudy Inst. Teor. Geofiz. Akad. Nauk SSSR. 1:95-115

Orszag SA (1970) Analytical theories of turbulence. Journal of Fluid Mechanics. 41(2):363-386

Ozmidov R (1965) On the turbulent exchange in a stably stratified ocean. Izv. Acad. Sci. USSR. Atmos. Oceanic Phys. 1:861-871

Persson POG, Fairall CW, Andreas EL, Guest PS and Perovich DK (2002) Measurements near the Atmospheric Surface Flux Group tower at SHEBA: Near‐surface conditions and surface energy budget. Journal of Geophysical Research: Oceans. 107(C10):SHE 21-21-SHE 21-35

Petenko I, Argentini S, Casasanta G, Genthon C and Kallistratova M (2018) Stable Surface-Based Turbulent Layer During the Polar Winter at Dome C, Antarctica: Sodar and In Situ Observations. Boundary-Layer Meteorology:1-28

Pope S (2000) Turbulent flows. Cambridge University Press, Cambridge, 771 pp

Saddoughi SG and Veeravalli SV (1994) Local isotropy in turbulent boundary layers at high Reynolds number. Journal of Fluid Mechanics. 268:333-372

Sakai Y, Uchida K, Kubo T and Nagata K (2008) Statistical features of scalar flux in a high-Schmidt-number turbulent jet. In: Kaneda Y (ed). IUTAM Symposium on Computational Physics and New Perspectives in Turbulence, 2008, Springer, Dordrecht, pp 209-214

Smedman A-S (1988) Observations of a multi-level turbulence structure in a very stable atmospheric boundary layer. Boundary-Layer Meteorology. 44(3):231-253

Stiperski I and Calaf M (2018) Dependence of near‐surface similarity scaling on the anisotropy of atmospheric turbulence. Quarterly Journal of the Royal Meteorological Society. 144(712):641-657

Stiperski I, Calaf M and Rotach MW (2019) Scaling, Anisotropy, and Complexity in Near-Surface Atmospheric Turbulence. Journal of Geophysical Research: Atmospheres. 124(3):1428-1448

Sukoriansky S, Kit E, Zemach E, Midya S and Fernando H (2018) Inertial range skewness of the longitudinal velocity derivative in locally isotropic turbulence. Physical Review Fluids. 3(11):114605

Taylor GI (1938) The spectrum of turbulence. Proceedings of the Royal Society of London A: Mathematical, Physical and Engineering Sciences. 164(919):476-490

Torrence C and Compo GP (1998) A practical guide to wavelet analysis. Bulletin of the American Meteorological society. 79(1):61-78

Townsend AA (1976) The structure of turbulent shear flow. Cambridge University Press, Cambridge and New York, 438 pp

Van Atta C and Chen W (1970) Structure functions of turbulence in the atmospheric boundary layer over the ocean. Journal of Fluid Mechanics. 44(1):145-159

Vercauteren N, Bou-Zeid E, Parlange MB, Lemmin U, Huwald H, Selker J and Meneveau C (2008) Subgrid-scale dynamics of water vapour, heat, and momentum over a lake. Boundary-Layer Meteorology. 128(2):205-228

Vignon E, Genthon C, Barral H, Amory C, Picard G, Gallée H, Casasanta G and Argentini S (2017a) Momentum-and Heat-Flux Parametrization at Dome C, Antarctica: A Sensitivity Study. Boundary-Layer Meteorology. 162(2):341-367

Vignon E, van de Wiel BJ, van Hooijdonk IG, Genthon C, van der Linden SJ, van Hooft JA, Baas P, Maurel W, Traullé O and Casasanta G (2017b) Stable boundary‐layer regimes at Dome C, Antarctica: observation and analysis. Quarterly Journal of the Royal Meteorological Society. 143(704):1241-1253

Waite ML (2011) Stratified turbulence at the buoyancy scale. Physics of Fluids. 23(6):066602

Watanabe T and Gotoh T (2007) Scalar flux spectrum in isotropic steady turbulence with a uniform mean gradient. Physics of Fluids. 19(12):121701

Wyngaard J and Coté O (1972) Cospectral similarity in the atmospheric surface layer. Quarterly Journal of the Royal Meteorological Society. 98(417):590-603